

7. Immerzeel, W. W., Droogers, P., de Jong, S. M. and Bierkens, M. F. P., Large-scale monitoring of snow cover and runoff simulation in Himalayan river basins using remote sensing. *Remote Sensing Environ.*, 2009, **113**(1), 40–49.
8. Dahe, Q., Shiyin, L. and Peiji, L., Snow cover distribution, variability, and response to climate change in western China. *J. Climate*, 2006, **19**, 1820–1833.
9. Pu, Z., Xu, L. and Salomonson, V., MODIS/Terra observed seasonal variations of snow cover over the Tibetan Plateau. *Geophys. Res. Lett.*, 2007, **34**, 1–6.
10. Wang, X., Xie, H. and Liang, T., Evaluation of MODIS snow cover and cloud mask and its application in Northern Xinjiang, China. *Remote Sensing Environ.*, 2008, **112**, 1497–1513.
11. Bookhagen, B. and Burbank, D. W., Toward a complete Himalayan hydrological budget: spatiotemporal distribution of snowmelt and rainfall and their impact on river discharge. *J. Geophys. Res.*, 2010, **115**, 1–25.
12. Kripalani, R. H., Kulkarni, A. and Sabade, S. S., Western Himalayan snow cover and Indian monsoon rainfall: A re-examination with INSAT and NCEP/NCAR data. *Theor. Appl. Climatol.*, 2003, **74**(1), 1–18.
13. Negi, H., Thakur, N., Kumar, R. and Kumar, M., Monitoring and evaluation of seasonal snow cover in Kashmir valley using remote sensing, GIS and ancillary data. *J. Earth System Sci.*, 2009, **118**(6), 711–720.
14. Kaur, R., Saikumar, D., Kulkarni, A. V. and Chaudhary, B. S., Variations in snow cover and snowline altitude in Baspa Basin. *Curr. Sci.*, 2009, **96**, 1255–1258.
15. Tekeli, A. E., Akyurek, Z., ArdaSorman, A., Sensoy, A. and Unal-Sorman, A., Using MODIS snow cover maps in modeling snowmelt runoff process in the eastern part of Turkey. *Remote Sensing Environ.*, 2005, **97**(2), 216.
16. Terzago, S., Cassardo, C., Cremonini, R. and Fratianni, S., Snow precipitation and snow cover climatic variability for the period 1971–2009 in the southwestern Italian Alps: The 2008–2009 snow season case study. *Water*, 2010, **2**(4), 773–787.
17. Zhang, Y., Yan, S. and Lu, Y., Snow cover monitoring using MODIS data in Liaoning Province, Northeastern China. *Remote Sensing*, 2010, **2**(3), 777–793.
18. Hall, D. K. and Riggs, G. A., Accuracy assessment of the MODIS snow products. *Hydrol. Process.*, 2007, **21**(12), 1534–1547.
19. Gafurov, A. and Bardossy, A., Cloud removal methodology from MODIS snow cover product. *Hydrol. Earth Syst. Sci.*, 2009, **13**(7), 1361–1373.
20. Kulkarni, A. V., Rathore, B. P., Singh, S. K. and Ajai, Distribution of seasonal snow cover in central and western Himalaya. *Ann. Glaciol.*, 2010, **54**, 123–128.
21. Jain, S., Goswami, A. and Saraf, A., Role of elevation and aspect in snow distribution in Western Himalaya. *Water Resour. Manage.*, 2009, **23**(1), 71–83.

ACKNOWLEDGEMENTS. This article is based on work supported by the Swedish International Development Cooperation Agency under the project. The temperature data from AWS data at Lunana, were made available by Karma Toeb, Department of Geology and Mines, Government of Bhutan. We thank our colleagues at ICIMOD, professionals from collaborating institutions, and independent experts who contributed significantly during various parts of the project. We also thank Gauri Dangol and Pradeep Dangol (ICIMOD) for help in analysing snow cover data and graphics work.

Received 26 September 2011; revised accepted 4 October 2011

Does carbonate ion control planktonic foraminifera shell calcification in upwelling regions?

Sushant S. Naik*, Shital P. Godad and P. Divakar Naidu

National Institute of Oceanography, Dona Paula, Goa 403 004, India

Planktonic foraminifera shell weights have been recognized as possible proxy for surface water carbonate ion concentration $[\text{CO}_3^-]$ and atmospheric CO_2 . However, to utilize this proxy, it is important to understand whether shell weights truly reflect surface water $[\text{CO}_3^-]$. We utilize shell weights of *Globigerina bulloides* and *Globigerinoides ruber* in the size range of 300 to 355 μm from a sediment core recovered from above the lysocline in the upwelling region of western Arabian Sea. Shell weights of *G. ruber* and *G. bulloides* show significant correlation with their shell size from recent to 16 kyr, which suggests that shell calcification was controlled by optimum growth conditions. On the other hand, during 16 to 22 kyr, there is no correlation between shell weights and shell size. However, shell weights of *G. bulloides* exhibit significant negative correlation with annual sea surface temperature which suggests that *G. bulloides* calcification might have been controlled by surface water $[\text{CO}_3^-]$. Therefore it is suggested here that shell weights of *G. ruber* and *G. bulloides* cannot be utilized to reconstruct surface water $[\text{CO}_3^-]$ in this region.

Keywords: Planktonic foraminifera, shell weights, upwelling, western Arabian Sea.

THE atmospheric carbon dioxide (CO_2) has fluctuated between ~180 and 280 ppm between the glacial and interglacials respectively¹. This atmospheric CO_2 is known to dissolve in surface seawater through physical-chemical reactions and affect the equilibrium between the ‘dissolved inorganic carbon (DIC)’ species; H_2CO_3 , HCO_3^- and CO_3^- . As CO_2 is absorbed by the ocean, it subsequently causes an increase in $[\text{H}^+]$, i.e. lowered pH and a decrease in carbonate ion concentration $[\text{CO}_3^-]$, which makes the seawater less alkaline. Lower seawater $[\text{CO}_3^-]$ is known to reduce the calcification rates of calcite-secreting organisms such as foraminifera². Planktonic foraminifera shell calcification and hence shell weights depend upon $[\text{CO}_3^-]$ of surface waters wherein they calcify^{3,4}. Drawing upon this trait, the shell weights of *G. sacculifer* were used to reconstruct $[\text{CO}_3^-]$ of surface waters in the Arabian Sea⁵.

The western Arabian Sea is a region of intense upwelling which makes it a strong CO_2 source to the atmosphere in the past and present. However, the CO_2 concentrations

*For correspondence. (e-mail: sushant@nio.org)

of surface water in the past have not been quantified. The shell weights of planktonic foraminifera could possibly be used to reconstruct $[\text{CO}_3^{2-}]$ of surface waters^{3,4}. However, there are studies which suggest that the controls on shell calcification are not $[\text{CO}_3^{2-}]$ but, it depends on optimum growth conditions of individual species^{6,7}. It was also shown that factors controlling shell calcification differ from species to species⁸. Yet another study suggest that shell weights are not controlled by $[\text{CO}_3^{2-}]$ nor do they depend on optimal growth conditions⁹. Thus, the controls over foraminifera shell calcification are still debated and to utilize shell weights of a particular species as a surface water carbonate ion proxy, it is important to understand whether $[\text{CO}_3^{2-}]$ controls shell calcification in that species over a period of time.

We therefore utilize the shell weights in the narrow size range of 300 to 355 μm of two planktonic foraminifera species, *Globigerina bulloides* and *Globigerinoides ruber* from a sediment core covering last 22 kyr. We attempt to evaluate whether surface water $[\text{CO}_3^{2-}]$ controls shell calcification of these two species during the glacial and interglacial in the upwelling region of the western Arabian Sea.

The western Arabian Sea is characterized by strong southwesterly monsoon winds during the northern hemisphere summer, which blow across the Arabian Sea, causing offshore Ekman transport and intense seasonal upwelling along the Oman and Somalia margins^{10–13}. The upwelling process brings cold, nutrient-rich waters from a few hundred metres depth to the surface and increases the biological productivity in the euphotic zone. These southwest (SW) monsoon winds and associated upwelling processes make the Arabian Sea one of the highest productive regions in the world oceans¹⁴. During the northeast (NE) monsoon the upwelling is suppressed¹⁵ but there is a convective mixing due to surface cooling¹⁶. However, a comparison of seasonal sea surface temperatures (SSTs) averaged for the period from 1970 to 2007 showed warmer SSTs during winter compared to those of the SW monsoon upwelled waters¹⁷ thus emphasizing the intensity of upwelling in this region.

Ocean Drilling Programme (ODP) Site 723A; location: $18^\circ 03' \text{N}$ and $57^\circ 37' \text{E}$, from the Oman margin at a water depth of 807.8 m was utilized for the present study (Figure 1). The age model for this site was based on AMS ^{14}C dates derived at 13 depth intervals of the sediment core¹⁸. The sediment samples were soaked in distilled water and wet sieved through a $>63 \mu\text{m}$ sieve. A portion of the coarse fraction ($>63 \mu\text{m}$) was sonicated in methanol for 8 s at 40 Hz to clean the shells. The cleaned shells were oven dried at 50°C and then sieved through a 300–355 μm size fraction. *G. bulloides* and *G. ruber* shells, about thirty in number, were picked from the 300–355 μm size fraction under a Stereo Binocular Microscope and weighed on a microbalance (1σ precision: $\pm 2 \mu\text{g}$, $n = 10$). Shell weight measurements were made on

core sections where at least 30 numbers of shells were available.

Carbonate ion concentration of bottom water at the core site was calculated using a programme designed by Taro Takahashi of Lamont Doherty Earth Observatory (pers. commun., 2006). The inputs for the programme were: depth, temperature, salinity, alkalinity, total CO_2 , silicate and phosphate. The *in situ* data was obtained from the US JGOFS database (cruise TTN-049 and station S2 close to the core site; location: $18^\circ 10' \text{N}$ and $58^\circ 01' \text{E}$).

The calculated pressure-normalized $[\text{CO}_3^{2-}]^*$ at a depth of 807.8 m is $132 \mu\text{mol kg}^{-1}$. This value is much higher than the threshold value of $105 \mu\text{mol kg}^{-1}$ below which dissolution of calcite begins¹⁹. Therefore it is expected that calcite dissolution at the core site is negligible.

Shell weights of *G. bulloides* and *G. ruber* range from ~ 7 to $\sim 20 \mu\text{g}$ and ~ 13 to $30 \mu\text{g}$ respectively over the last 22 kyr, at ODP Site 723A (Figure 2a and b; Table 1). The shell weights of both these species showed a significant correlation to each other for the entire record ($r = 0.66$, $n = 21$; 99.5% significance level). Over the last 22 kyr, there was a distinct transition in atmospheric CO_2 (ref. 20) and temperature at ~ 16 kyr (Figure 2c). The recent to 16 kyr and 16–22 kyr represent the warm and cold periods respectively. During recent to 16 kyr, *G. bulloides* recorded an average weight of $11.6 \mu\text{g}$ and during 16–22 kyr the average shell weight was $12 \mu\text{g}$, whereas *G. ruber* weighed an average of $17.5 \mu\text{g}$ and $20.9 \mu\text{g}$ during the respective periods (Figure 2a and b). Thus, the average shell weight of both the species was lower during recent to 16 kyr than during 16–22 kyr. A

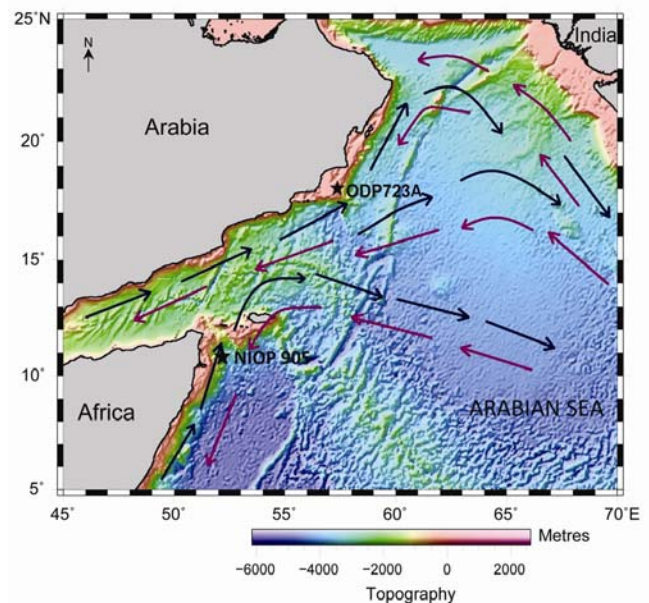


Figure 1. Map showing location of ODP Site 723 analysed in this study. Blue arrows show surface water circulation (SWC) during southwest monsoon and pink arrows show SWC during northeast monsoon. Site NIOP 905 is shown for comparison (see text).

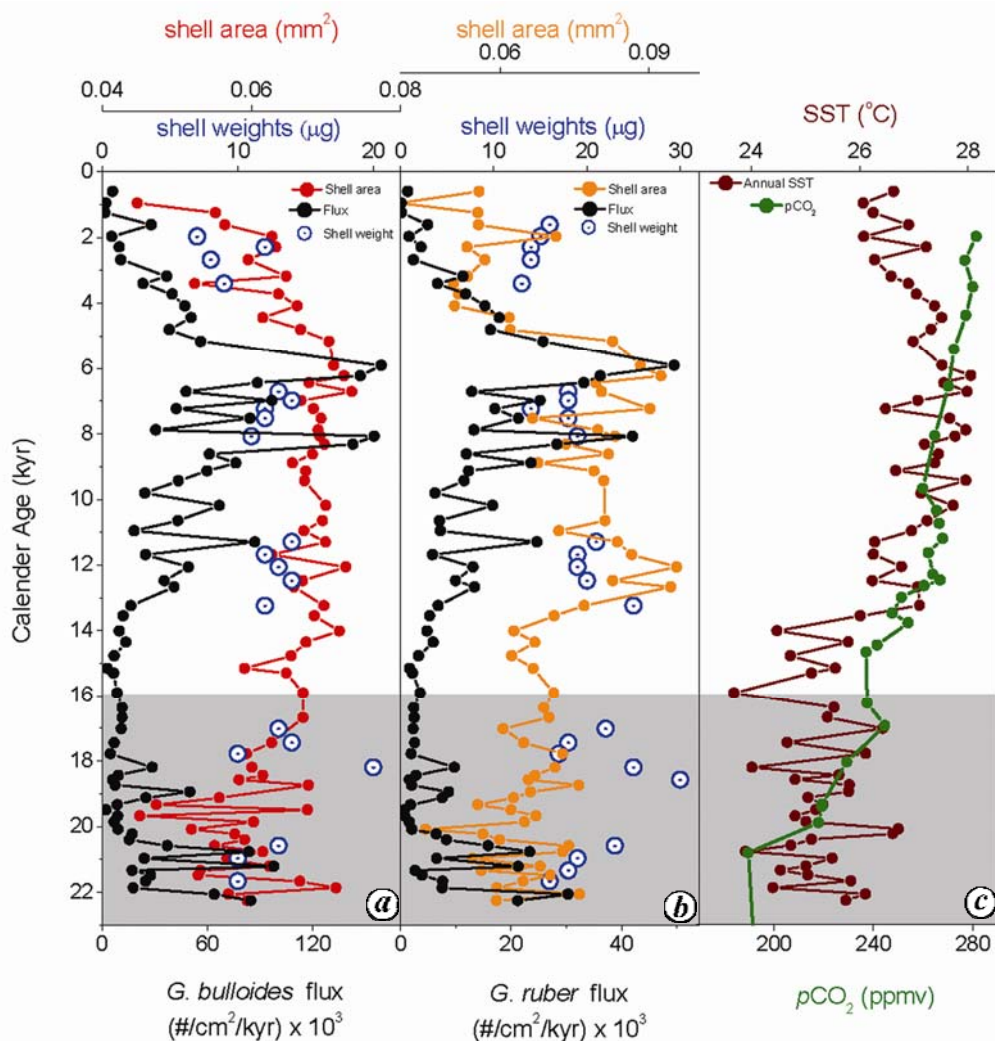


Figure 2. Down-core variations in shell weights, flux and shell area (mm^2) for the planktonic foraminifera species, (a) *G. bulloides*, (b) *G. ruber* and (c) annual sea surface temperature estimates from ODP Site 723 and atmospheric CO_2 obtained from an Antarctic ice core²⁰. Shaded region marks the colder period (16–22 kyr).

study²¹ at Site NIOP 905 in the Arabian Sea (Figure 1) reports *G. ruber* shell weight averages of 15.7 μg and 19.7 μg (size range of 300–355 μm) during the Holocene and Last Glacial Maximum (LGM) respectively and is in close comparison to our study.

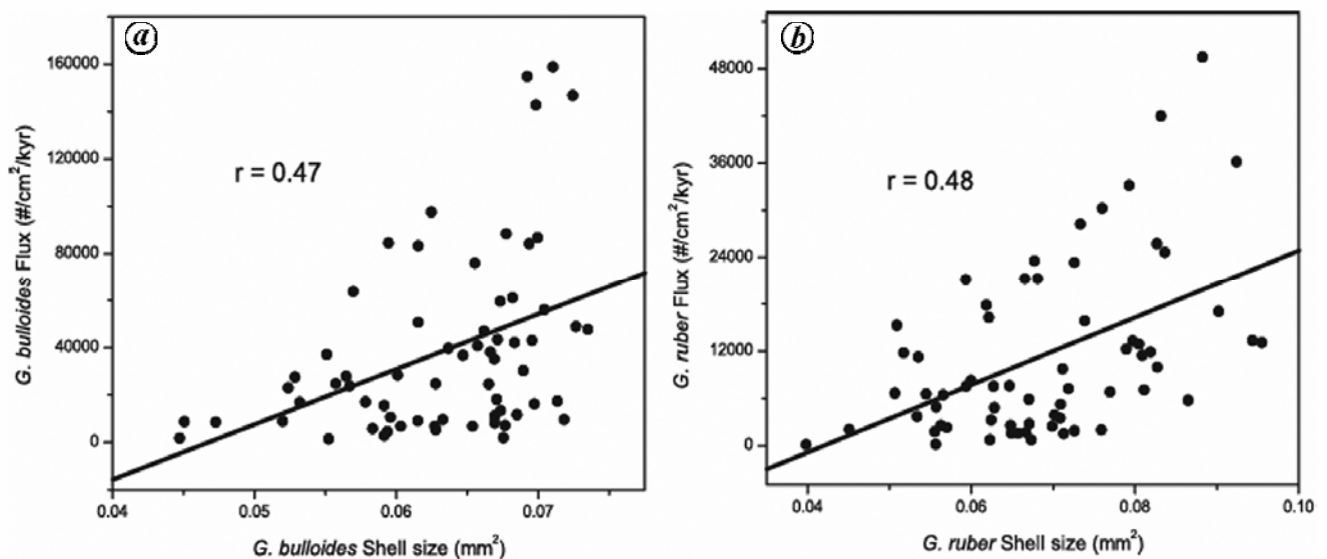
G. bulloides and *G. ruber* were selected based on their attuning to different environmental conditions. *G. bulloides* is better resistant to dissolution in comparison to *G. ruber*. *G. bulloides* is a sub-polar species whereas *G. ruber* is a sub-tropical species. It was shown that the maximum occurrence of *G. bulloides* was associated with greater nutrient concentrations and lower SSTs during the SW monsoon upwelling period in the Arabian Sea^{22,23}. On the other hand, *G. ruber* occurs throughout the year with high abundances during the SW monsoon followed by NE monsoon period^{15,24,25}. Further, *G. bulloides* is a symbiont-bearing species and *G. ruber* is a symbiont-bearing species. The symbionts elevate the pH, CO_3^- and O_2 levels close to

the foraminiferal test wall and maybe responsible in influencing the shell size and weight⁹. Additionally, *G. bulloides* and *G. ruber* do not secrete gametogenic calcite²⁶. Therefore, a comparison between *G. bulloides* and *G. ruber* will help in understanding shell calcification in symbiont and non-symbiont species.

Significant positive correlation between shell weights of *G. bulloides* and *G. ruber* suggests that shell calcification is controlled by common factors for both the species. Upwelling indices such as fluxes, total planktonic foraminifera and relative abundance of *G. bulloides* inferred that the intensity of upwelling in the western Arabian Sea was stronger during Holocene than in the last glacial period²⁷. It was seen that larger shells were produced (measured in terms of area in mm^2) during strong upwelling period and smaller mean test sizes were produced during the last glacial period when the upwelling was comparatively weaker and inferred that nutrient-rich

Table 1. Shell weights and shell sizes of *Globigerina bulloides* and *Globigerinoides ruber* and annual sea surface temperature (SST) from ODP core 723A

Age (kyr)	Shell weights of <i>G. bulloides</i> (μg)	Shell weights of <i>G. ruber</i> (μg)	Shell size of <i>G. bulloides</i> (mm^2)	Shell size of <i>G. ruber</i> (mm^2)	Annual SST ($^{\circ}\text{C}$)
1.61	–	16	0.05645	0.05569	26.90
1.97	7	15	0.06277	0.07126	26.08
2.29	12	14	0.06326	0.05336	27.23
2.68	8	14	0.05958	0.057	26.27
3.4	9	13	0.05238	0.05065	26.90
6.72	13	18	0.07347	0.08046	27.98
6.99	14	18	0.06666	–	27.07
7.24	12	14	0.06831	0.09021	26.48
7.53	12	18	0.06934	0.06654	27.66
8.08	11	19	0.06921	0.08316	27.76
11.3	14	21	0.06992	0.08365	26.28
11.68	12	19	0.06275	0.08648	26.25
12.06	13	19	0.07264	0.09551	26.77
12.48	14	20	0.06689	0.08269	26.23
13.24	12	25	0.06972	0.07696	27.11
17.02	13	22	0.06772	0.06065	26.43
17.44	14	18	0.0627	0.06478	24.66
17.78	10	17	0.05935	0.0726	26.11
18.2	20	25	0.06009	0.07111	24.01
18.57	–	30	0.05833	0.06573	24.81
20.58	13	23	0.05509	0.07385	24.73
20.97	10	19	0.05671	0.05448	25.50
21.34	–	18	0.05317	0.05625	24.54
21.48	–	–	0.05285	0.07015	25.04
21.67	10	16	0.0665	0.06463	25.84

**Figure 3.** Scatter plots showing correlation between shell weight and shell size of (a) *G. bulloides* and (b) *G. ruber*.

upwelled waters would provide optimum environment for planktonic foraminifera to grow to a larger size²⁸. Shell weights of *G. bulloides* and *G. ruber* were compared with the shell sizes of these species obtained from the same core²⁸ (Figure 2 a and b). During recent to 16 kyr, shell size was significantly correlated to flux for both species, *G. bulloides* ($r = 0.47$, $n = 39$; 99.5% significance level,

Figure 3 a) and *G. ruber* ($r = 0.48$, $n = 39$; 99.5% significance level, Figure 3 b). Further, shell size and weights of *G. bulloides* show a significant correlation during recent to 16 kyr ($r = 0.65$, $n = 14$; 99.5% significance level). The same is observed for shell size and shell weights of *G. ruber* ($n = 0.55$, $n = 15$; 97.5% significance level). Thus it is seen that during recent to 16 kyr calcification

rates of planktonic foraminifera are proportional to the upwelling intensity at this site. During intense upwelling periods the conditions were favourable for *G. bulloides* and *G. ruber* to proliferate and the flux, shell size and shell weights of this species increased.

Comparison of *G. bulloides* and *G. ruber* flux, their shell sizes and shell weights do not show significant correlations during 16–22 kyr. There is a distinct decrease in average shell size of both the species during 16–22 kyr compared to the recent to 16 kyr period. However, during 16–22 kyr, shell weights of both the species increase which indicates that factors other than optimum growth conditions are responsible in controlling shell calcification during the colder period.

It should be noted that at the present site, surface waters are not in equilibrium with the atmospheric CO₂ due to intense upwelling. On the contrary, the Arabian Sea was a continuous source of CO₂ to the atmosphere at least throughout the past 30 kyr as a result of upwelling^{29,30}. The upwelled waters have lower temperatures, higher CO₂ and hence lower CO₃²⁻ concentrations. If [CO₃²⁻] was the factor controlling shell calcification during recent to 16 kyr, shell weights should have been lowest during periods of intense upwelling which is contrary to our observations.

Other possible factor controlling shell calcification is temperature⁸. To understand the temperature control on shell calcification, we compared the sediment core shell weights with annual SST estimates, reconstructed using artificial neural networks, based on quantitative analyses of planktonic foraminifera¹⁸ (Table 1). During recent to 16 kyr, the correlations between shell weights of *G. bulloides* and annual temperature ($r = 0.24$, $n = 14$) as well as *G. ruber* and annual temperature ($r = 0.12$, $n = 15$) are insignificant. On the other hand, during 16 to 22 kyr, a significant correlation with temperature was seen for *G. bulloides* ($r = -0.76$, $n = 7$; 97.5% significance level) and an insignificant correlation with *G. ruber* ($r = -0.4$, $n = 9$). This indicates, colder temperatures within the last glacial periods were conducive to produce thicker *G. bulloides* shells. The *G. ruber* shell weight correlation with annual temperature is negative but not significant and the reasons for this behaviour are uncertain. Colder waters dissolve more CO₂ and lower the surface water [CO₃²⁻] and hence should have produced lighter *G. bulloides* shells, which is in contrast to our observations. Therefore, the effect of temperature on shell calcification can be ruled out. The variability of shell weights within the glacial period seems to be controlled by atmospheric CO₂ which was lower during the last glacial period, which in turn lead to a higher surface water [CO₃²⁻] and hence produced heavier shells. Thus, it is seen in the present study that during recent to 16 kyr, shell weights are controlled by optimum growth conditions whereas during the glacial period, surface water [CO₃²⁻] is a possible controlling factor.

The following conclusions emerge from this study:

(1) During recent to 16 kyr shell weights of *G. bulloides* and *G. ruber* were correlated to shell size which suggests that shell calcification was controlled by optimum growth conditions driven by intense upwelling.

(2) During 16 to 22 kyr, shell weights of *G. bulloides* were not correlated to shell sizes but showed a significant negative correlation with annual SSTs which suggests that surface water [CO₃²⁻] may have controlled shell calcification of *G. bulloides*.

Thus, the present study reveals that different factors may control planktonic foraminifera shell calcification over a period of time. Therefore foraminifera shell weights of *G. bulloides* and *G. ruber* cannot be utilized as a proxy of surface water [CO₃²⁻] in the upwelling region of the Arabian Sea.

- Petit, J. R. *et al.*, Climate and atmospheric history of the past 420,000 years from the Vostok ice core, Antarctica. *Nature*, 1999, **399**, 429–436.
- Bijma, J., Spero, H. J. and Lea, D. W., Reassessing foraminiferal stable isotope geochemistry: Impact of the oceanic carbonate system. In *Use of Proxies in Paleoceanography: Examples of the South Atlantic* (eds Fisher, G. and Wefer, G.), Springer-Verlag, New York, 1999, pp. 489–512.
- Barker, S. and Elderfield, H., Foraminiferal calcification response to glacial–interglacial changes in atmospheric CO₂. *Science*, 2002, **297**, 833–836.
- Naik, S. S. and Naidu, P. D., Calcite dissolution along a transect in the western tropical Indian Ocean: a multiproxy approach. *Geochem. Geophys. Geosys.*, 2007, **8**, Q08009; doi:10.1029/2007GC001615.
- Naik, S. S., Naidu, P. D., Govil, P. and Godad, S., Relationship between weights of planktonic foraminifer shell and surface water CO₃²⁻ concentration during the Holocene and Last Glacial Period. *Mar. Geol.*, 2010, **275**, 278–282.
- de Villiers, S., A 425 ka record of foraminiferal shell weight variability in the western Equatorial Pacific. *Paleoceanography*, 2003, **18**(3), 1080.
- de Villiers, S., Occupation of an ecological niche as the fundamental control on the shell-weight of calcifying planktonic foraminifera. *Mar. Biol.*, 2004, **144**(1), 45–50.
- Gonzalez-Mora, B., Sierro, F. J. and Flores, J. A., Controls of shell calcification in planktonic foraminifers. *Quaternary Sci. Rev.*, 2008, **27**, 956–961.
- Beer, C. J., Schiebel, R. and Wilson, P. A., Testing planktonic foraminiferal shell weight as a surface water [CO₃²⁻] proxy using plankton net sample. *Geology*, 2010, **38**(2), 103–106; doi: 10.1130/G30150.1.
- Wyrski, K., Physical oceanography of the Indian Ocean. In *The Biology of the Indian Ocean* (ed. Zeitzschelp, B.), Springer-Verlag, New York, 1973, pp. 18–36.
- Schott, F., Monsoon response of the Somalia Current and associated upwelling. *Progr. Oceanogr.*, 1983, **12**, 357–382.
- Shallow, J. C., Some aspects of the physical oceanography of the Indian Ocean. *Deep-Sea Res. Part A*, 1984, **31**, 639–650.
- Bauer, S., Hitchcock, G. L. and Olson, D. B., Influence of monsoon-forced Ekman dynamics upon surface layer depth and plankton biomass distribution in the Arabian Sea. *Deep-Sea Res. Part A*, 1991, **38**, 531–553.
- Qasim, S. Z., Oceanography of the northern Arabian Sea. *Deep-Sea Res. Part A*, 1982, **29**, 1041–1068.

15. Curry, W. B., Osterman, D. R., Guptha, M. V. S. and Ittekkot, V., Foraminiferal production and monsoonal upwelling in the Arabian Sea: Evidence from sediment traps. In *Upwelling Systems; Evolution Since the Early Miocene* (eds Summerhays, C. P., Prell, W. L. and Emeis, K. C.), Geological Society of London, London, 1992, pp. 93–106.
16. Madhupratap, M., Kumar, S. P., Bhattathiri, P. M. A., Kumar, M. D., Raghukumar, S., Nair, K. K. C. and Ramaiah, N., Mechanism of the biological response to winter cooling in the Arabian Sea. *Nature*, 1996, **384**, 549–551.
17. Takahashi, T. *et al.*, Climatological mean and decadal changes in surface ocean pCO₂, and net sea-air CO₂ flux over the global oceans. *Deep-Sea Res. II*, 2009, **56**, 554–577.
18. Naidu, P. D. and Malmgren, B. A., Seasonal sea surface temperature contrast between the Holocene and last glacial period in the western Arabian Sea (Ocean Drilling Project Site 723A): Modulated by monsoon upwelling. *Paleoceanography*, 2005, **20**, PA1004; doi:10.1029/2004PA001078.
19. Broecker, W. S. and Clark, E., CaCO₃ size distribution: A paleo-carbonate ion proxy. *Paleoceanography*, 1999, **14**, 596–604.
20. Smith, H. J., Fischer, H., Wahlen, M., Mastroianni, D. and Deck, B., Dual modes of the carbon cycle since the Last Glacial Maximum. *Nature*, 1999, **400**, 248–250.
21. de Moel, H., Ganssen, G. M., Peeters, F. J. C., Jung, S. J. A., Kroon, D., Brummer, G. J. A. and Zeebe, R. E., Planktic foraminiferal shell thinning in the Arabian Sea due to anthropogenic ocean acidification? *Biogeosciences*, 2009, **6**, 1917–1925.
22. Prell, W. L., Monsoonal climate of the Arabian Sea during the late Quaternary: a response to changing solar radiation. In *Milankovitch and Climate* (eds Berger, A. L. *et al.*), D. Reidel, Dordrecht, 1984, pp. 349–366.
23. Brock, J. C., McClain, C. R., Anderson, D. M. and Hay, W. W., South west monsoon circulation and environments of recent planktonic foraminifera in the NW Arabian Sea. *Paleoceanography*, 1992, **7**, 799–814.
24. Conan, S. M.-H., Ivanova, E. M. and Brummer, G.-J. A., Quantifying carbonate dissolution and calibration of foraminiferal dissolution indices in the Somali Basin. *Mar. Geol.*, 2002, **182**(3–4), 325–349.
25. Peeters, F. J. C., Brummer, G.-J. A. and Ganssen, G., The effect of upwelling on the distribution and stable isotope composition of *Globigerina bulloides* and *Globigerinoides ruber* (planktic foraminifera) in modern surface waters of the NW Arabian Sea. *Glob. Planet. Change*, 2002, **34**(3–4), 269–291.
26. Hemleben, C. and Spindler, M., Recent advances in research on living planktonic foraminifera. *Utrecht Micropal. Bull.*, 1983, **30**, 141–170.
27. Naidu, P. D. and Malmgren, B. A., A high-resolution record of late Quaternary upwelling along the Oman Margin, Arabian Sea based on planktonic foraminifera. *Paleoceanography*, 1996, **11**, 129–140.
28. Naidu, P. D. and Malmgren, B. A., Monsoon upwelling effects on test size of some planktonic foraminiferal species from the Oman Margin, Arabian Sea. *Paleoceanography*, 1995, **10**, 117–122.
29. Sabine, C. L., Wanninkhof, R., Key, R. M., Goyet, C. and Millero, F. J., Seasonal CO₂ fluxes in the tropical and subtropical Indian Ocean. *Mar. Chem.*, 2000, **72**, 33–53.
30. Palmer, M. R. *et al.*, Multi-proxy reconstruction of surface water pCO₂ in the northern Arabian Sea since 29 ka. *Earth Planet. Sci. Lett.*, 2010, **295**, 49–57.

ACKNOWLEDGEMENTS. We thank Dr S. Shetye, Director, National Institute of Oceanography for support and encouragement. Comments by two anonymous reviewers are highly appreciated. We also thank Ms Rubina Pednekar for laboratory assistance. We acknowledge the financial support of ISRO-GBP. A set of samples was provided by the Ocean Drilling Programme, which is sponsored by the US National Science Foundation and participating countries under the management of the Joint Oceanographic Institutions. This is NIO contribution number 5081.

Received 23 May 2011; revised accepted 31 October 2011